Finite Element Analysis of Crack Welding Process

Thomas Jin-Chee Liu

Abstract—The numerical simulation of the crack welding process is reported in this paper. The thermo-electro-structural coupled-field finite element analysis is adopted to investigate the welding process of crack surfaces. In the simulation, the pressure-dependent and temperature-dependent electrical contact conditions are considered. From the results, the crack surfaces can melt and weld together under the compressive load and electric current. The contact pressure effect must be considered in the finite element analysis to obtain more practical results.

Keywords—Crack welding, contact pressure, Joule heating, finite element, coupled-field.

I. INTRODUCTION

DUE to the Joule heating effect, hot regions at the crack tip or crack surface can be induced under the compressive load and electric current. Many studies have reported that the Joule heating effect can induce local compressive thermoelastic stresses and melting area at the crack tip arresting crack propagation [1]-[6].

Similar to the resistance spot welding process, the crack surfaces can melt and weld together under the Joule heating. In this paper, the crack welding process will be studied by the thermo-electro-structural finite element analyses with the software ANSYS 14.0. Based on the author's previous studies [7]-[9], the crack contact conditions are considered in the simulations. The temperature fields will be obtained for estimating the crack welding behaviors.

II. CASE STUDY

Fig. 1 shows the configuration of the case study. A metal plate with a central crack is subjected to the compressive force F_0 and DC current i_0. This thin plate is made of mild steel with dimensions $2W \times 2L \times e$. The crack length is $2a$. The thermo-electro-structural coupled-field problem in Fig. 1 will be solved by the finite element method. The plane stress, two-dimensional thermo-electric conditions, and isotropic properties are assumed. To simulate more practical conditions, the temperature-dependent material properties in Table I [10] are adopted in the analysis. Also, the elasto-plastic stress-strain properties in Fig. 2 are considered. The electric-current-induced thermo-structural problem is transient. The initial temperature is 21°C. From the conclusion of Liu [8], the phase change effect can be ignored.

The electrical-thermal-mechanical contact conditions

Thomas Jin-Chee Liu, Associate Professor, is with the Department of Mechanical Engineering, Ming Chi University of Technology, Taishan, New Taipei City, Taiwan (phone: 886-2-29089899 ext 4569; e-mail: jinchee@mail.mcut.edu.tw).

between crack surfaces are considered in this study. The electric current and heat flow can pass through the crack surfaces when the crack contact occurs. Fig. 3 shows the pressure-dependent and temperature-dependent electrical contact conditions considered in the simulations [11]. The symbol η_{cel} is the electrical conductance of the contact surfaces.
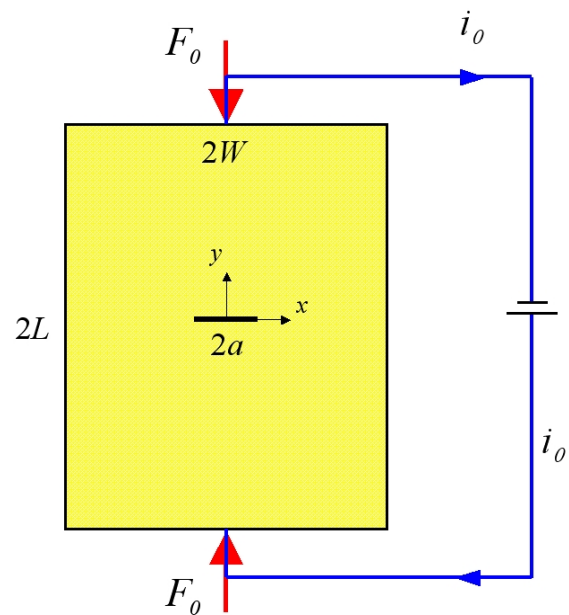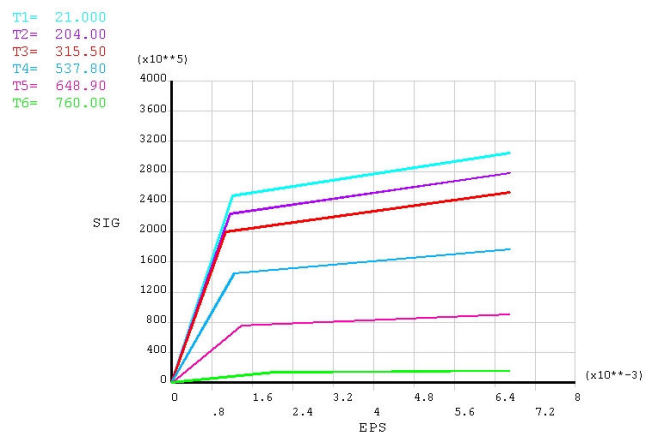

Fig. 1 Configuration and sample

Fig. 2 Elasto-plastic stress-strain

World Academy of Science, Engineering and Technology
International Journal of Mechanical and Mechatronics Engineering
Vol:8, No:1, 2014

TABLE I
TEMPERATURE-DEPENDENT PROPERTIES OF MILD STEEL [10]

Temperature (°C)	Young's modulus E (GPa)	Yielding strength S_Y (MPa)	Coefficient of thermal expansion α (1/°C)	Thermal conductivity k (W/ m-°C)	Specific heat C_p (J/ kg-°C)	Resistivity ρ (Ω-m)
21	206.8	248	10.98×10^{-6}	64.60	444	0.14224×10^{-6}
93	196.5	238	11.52×10^{-6}	63.15	452.38	0.18644×10^{-6}
204	194.4	224	12.24×10^{-6}	55.24	511.02	0.26670×10^{-6}
315.5	186	200	12.96×10^{-6}	49.87	561.29	0.37592×10^{-6}
426.7	169	173	13.50×10^{-6}	44.79	611.55	0.49530×10^{-6}
537.8	117	145	14.04×10^{-6}	39.71	661.81	0.64770×10^{-6}
648.9	55	76	14.58×10^{-6}	34.86	762.34	0.81788×10^{-6}
760	6.9	14	14.05×10^{-6}	30.46	1005.3	1.0109×10^{-6}
871	–	–	13.05×10^{-6}	28.37	1005.3	1.1151×10^{-6}
982	–	–	–	27.62	1005.3	1.1582×10^{-6}
1093	–	–	–	28.52	1189.6	1.1786×10^{-6}
1204	–	–	–	–	1189.6	1.2090×10^{-6}

* Poisson's ratio $\nu = 0.3$, density $\beta = 7861.2$ kg/m³, melting point = 1521 °C.
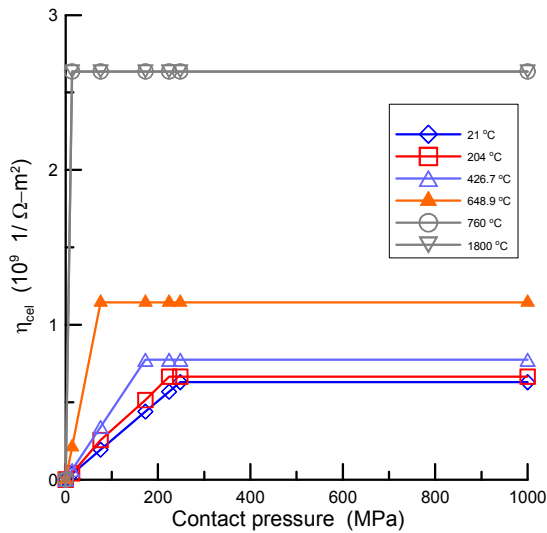

Fig. 3 Pressure-dependent and temperature-dependent electrical contact conditions
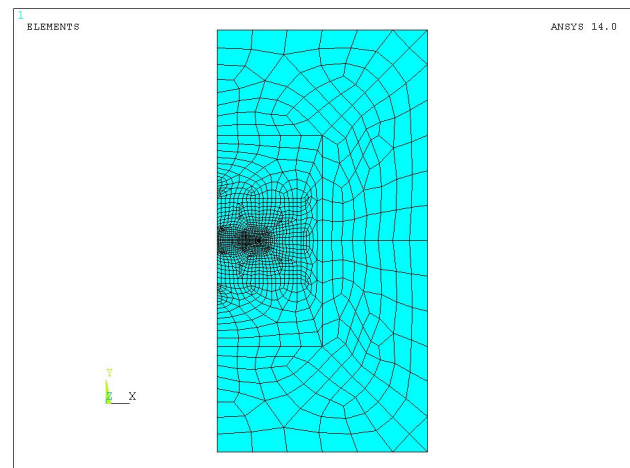
III. METHODS OF ANALYSES

In this study, the finite element equations of the thermo-electro-structural coupled-field analysis are listed as follows [12]:

$$\begin{bmatrix} \mathbf{M} & 0 & 0 \\ 0 & 0 & 0 \\ 0 & 0 & 0 \end{bmatrix}\begin{bmatrix} \ddot{\mathbf{U}} \\ \ddot{\mathbf{T}} \\ \ddot{\mathbf{V}} \end{bmatrix} + \begin{bmatrix} \mathbf{C} & 0 & 0 \\ \mathbf{C}^{tu} & \mathbf{C}^t & 0 \\ 0 & 0 & 0 \end{bmatrix}\begin{bmatrix} \dot{\mathbf{U}} \\ \dot{\mathbf{T}} \\ \dot{\mathbf{V}} \end{bmatrix} + \begin{bmatrix} \mathbf{K} & \mathbf{K}^{ut} & 0 \\ 0 & \mathbf{K}^t & 0 \\ 0 & 0 & \mathbf{K}^v \end{bmatrix}\begin{bmatrix} \mathbf{U} \\ \mathbf{T} \\ \mathbf{V} \end{bmatrix} = \begin{bmatrix} \mathbf{F} \\ \mathbf{Q} \\ \mathbf{I} \end{bmatrix} \quad (1)$$

where $\mathbf{U}$, $\mathbf{T}$, $\mathbf{V}$, $\mathbf{F}$, $\mathbf{Q}$ and $\mathbf{I}$ are the vector forms of the displacement, temperature, electric potential, force, heat flow rate and electric current, respectively. The material constant matrices $\mathbf{M}$, $\mathbf{C}$, $\mathbf{C}^t$, $\mathbf{C}^{tu}$, $\mathbf{K}$, $\mathbf{K}^t$, $\mathbf{K}^{ut}$ and $\mathbf{K}^v$ are the structural mass, structural damping, thermal specific heat, thermo-structural damping, structural stiffness, thermal conductivity, thermo-structural stiffness and electric conductivity, respectively. The coupled heat flow matrix $\mathbf{Q}$ contains the effects of the thermal loading and electrical Joule heating. $\mathbf{C}^{tu}$

and $\mathbf{K}^{ut}$ are thermo-structural coupled terms. Equation (1) is a directly coupled nonlinear equation which is solved using the Newton-Raphson iterative method.

The finite element model of the previous study [7] is adopted in this paper. The accuracy of the mesh has been validated by Liu [7]. Fig. 4 shows the finite element mesh of ANSYS with $W=L=0.05$ m and $a=0.01$ m. Due to the symmetry of the problem, only a half plate of Fig. 1 is analyzed. The symmetric conditions are applied on the finite element model. The plate is modeled by ANSYS element type: PLANE223, i.e. the 8-node isoparametric plane element with the thermo-electro-structural coupled-field analysis. The plane stress option is used due to the thin thickness ($e=0.001$ m). In Fig. 4, the model has 1822 elements and 5353 nodes. The quarter-point elements (QPE) [13] are used for modeling the $r^{-1/2}$ singularity at the crack tip.
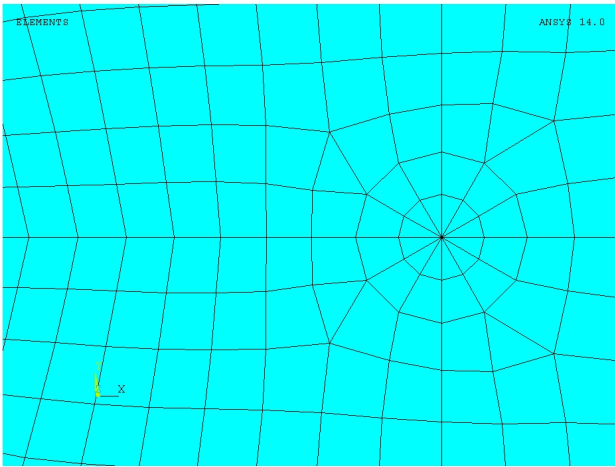

(a)

World Academy of Science, Engineering and Technology
International Journal of Mechanical and Mechatronics Engineering
Vol:8, No:1, 2014

(b)

Fig. 4 Finite element model (a) half model (b) local mesh

IV. RESULTS AND DISCUSSIONS

A. Hot Regions Due to Joule Heating

To investigate the temperature field on the plate, the external loads i_0=25000 A and F_0=0 N are applied on the plate boundary. The total operating time is 0.06 s. As a result, Fig. 5 shows that the temperature at the crack tip increases with time. In Fig. 6, it can be seen that the Joule heating effect causes a high temperature area at the crack tip. It demonstrates the existence of the melting crack tip (red color area) when enough electrical energy is provided.

In Fig. 7, the electric current density near the crack tip at t = 0.06 s is plotted. Due to the opening condition of the crack, the electric current density vectors cannot pass through the crack surfaces. It is noted that there is a field concentration at the crack tip. Similar to the elastic stress field, the electric current density also has the $r^{-1/2}$ singularity at the crack tip. Under the Joule heating effect, this current density concentration induces the hot spot around the crack tip (Fig. 6).
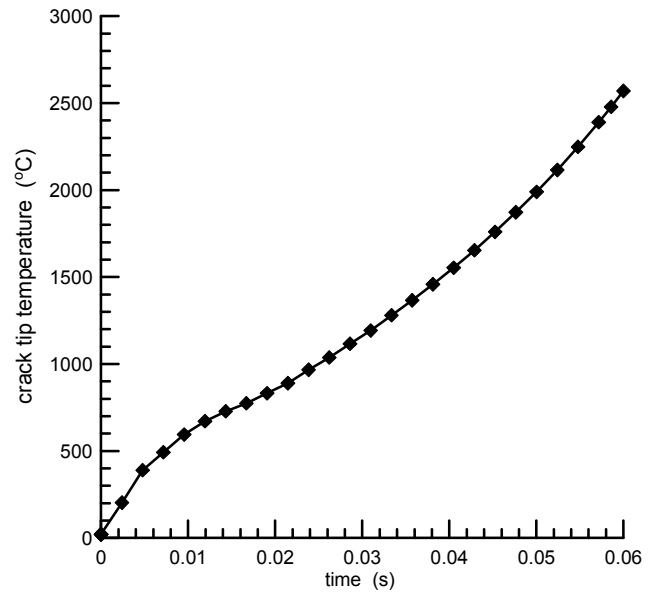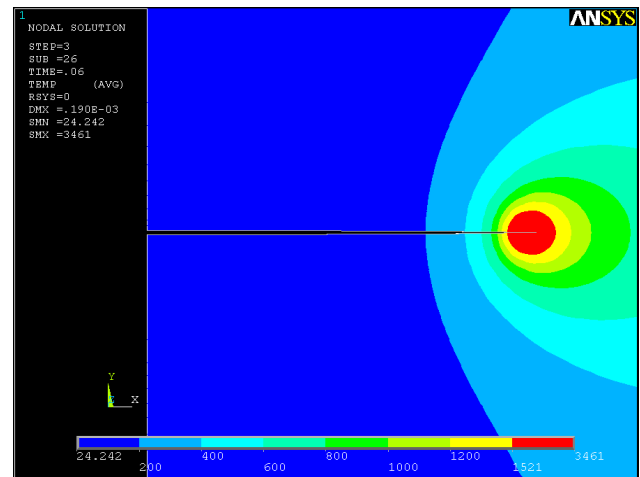

Fig. 5 Crack tip temperature
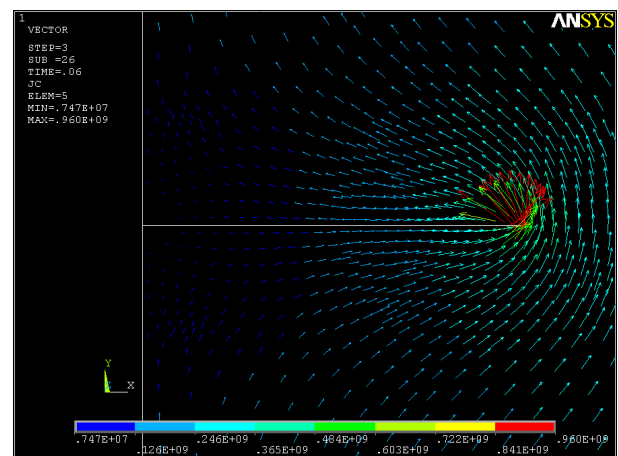

Fig. 6 Temperature contour

Fig. 7 Electric current density vectors

World Academy of Science, Engineering and Technology
International Journal of Mechanical and Mechatronics Engineering
Vol:8, No:1, 2014

B. Crack Contact and Crack Welding

To achieve the crack welding, the compressive force F_0 must be used so that the crack surfaces can contact together. Then the electric current can pass through the crack and the Joule heating effect can induce a hot region along the crack.
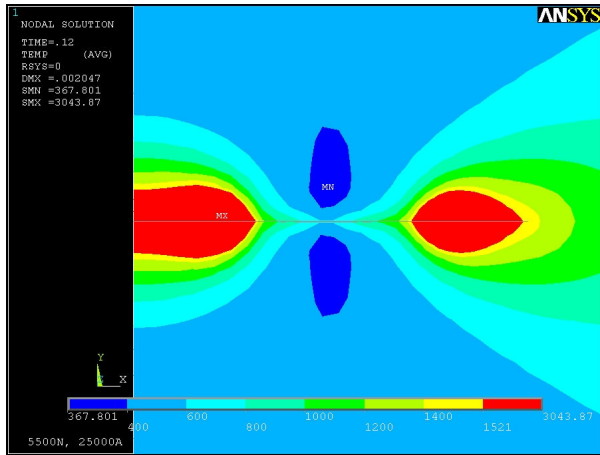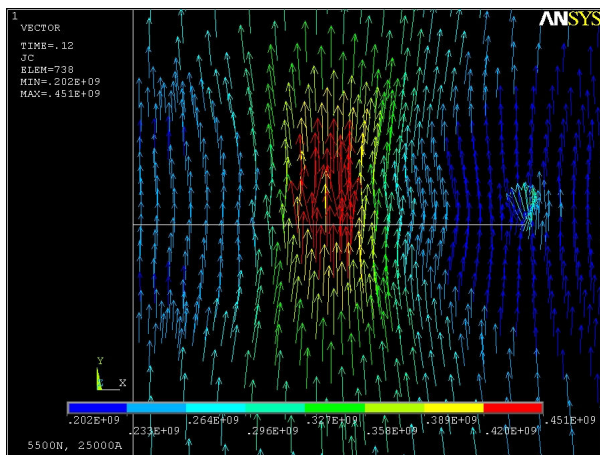

Fig. 8 Crack welding
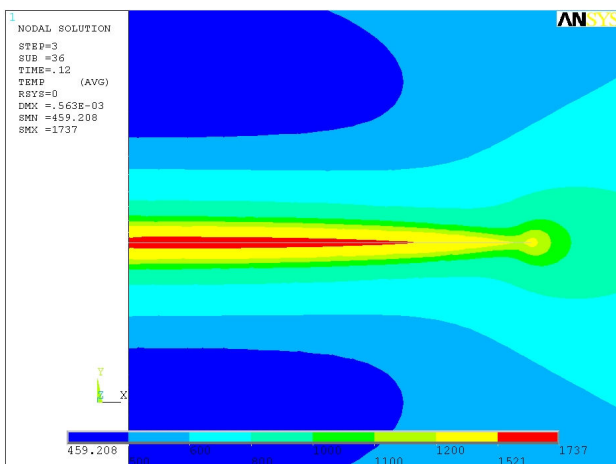

Fig. 9 Electrical contact

Fig. 10 Result from constant η_{cel}

The external loads i_0=25000 A and F_0=5500 N are applied on the plate boundary. The numerical result in Fig. 8 shows the temperature field and melted region (red color area). In Fig. 9, the electric current density vectors can pass through the crack. Due to the remote compressive load, the crack faces contact to each other. Similar to the resistance spot welding process, the crack surfaces can melt and weld together.

If the constant η_{cel} is used in the analysis, the result in Fig. 10 is obtained. Comparing Figs. 8 and 10, these two results are different. The result of Fig. 8 is more practical because the electrical contact conductance is pressure-dependent and temperature-dependent.

V. CONCLUSIONS

To achieve the crack welding, the compressive force must be used so that the crack surfaces can contact together. Also, the contact pressure effect (pressure-dependent and temperature-dependent η_{cel}) must be considered in the finite element analysis to obtain more practical results.

REFERENCES

[1] Kudryavtsev BA, Parton VZ and Rubinskii BD. Electromagnetic and thermoelastic fields in a conducting plate with a cut of finite length. Solids. Mech. 17, pp. 110–118, 1982.
[2] Parton VZ and Kudryavtsev BA. Electromagnetoelasticity. Gordon and Breach, New York, 1988.
[3] Cai GX and Yuan FG. Electric current-induced stresses at the crack tip in conductors. Int. J. Fract. 96, pp. 279–301, 1999.
[4] Fu YM, Bai XZ, Qiao GY, Hu YD and Luan JY. Technique for producing crack arrest by electromagnetic heating. Mater. Sci. Tech. 17, pp. 1653–1656, 2001.
[5] Hasanyan D, Librescu L, Qin Z and Young RD. Thermoelastic cracked plates carrying nonstationary electrical current. J. Therm. Stress. 28, pp. 729–745, 2005.
[6] Qin Z, Librescu L and Hasanyan D. Joule heating and its implications on crack detection/arrest in electrically conductive circular cylindrical shells. J. Therm. Stress. 30, pp. 623–637, 2007.
[7] Liu TJC. Thermo-electro-structural coupled analyses of crack arrest by Joule heating. Theor. Appl. Fract. Mech. 49, pp. 171–184, 2008.
[8] Liu TJC. Finite element modeling of melting crack tip under thermo-electric Joule heating. Engng. Fract. Mech. 78, pp. 666–684, 2011.
[9] Liu TJC. Fracture mechanics of steel plate under Joule heating analyzed by energy density criterion. Theor. Appl. Fract. Mech. 56, pp. 154–161, 2011.
[10] Tsai CL, Dai WL, Dickinson DW and Papritan JC. Analysis and development of a real-time control methodology in resistance spot welding. Weld. J. 70, pp. s339–351, 1991.
[11] Sun X and Dong P. Analysis of aluminum resistance spot welding processes using coupled finite element procedures. Weld. J. 79, pp. s215–s221, 2000.
[12] ANSYS, Inc.. ANSYS 14.0 Mechanical APDL Theory Reference. SAS IP, Inc., USA, 2011.
[13] Barsoum RS. On the use of isoparametric finite elements in linear fracture mechanics. Int. J. Numer. Meth. Eng. 10, pp. 25–37, 1976.